Supplementary Material

Transition Metal-Doped Porous Carbon Nitride Composite Serve as a Highly Reactive Catalyst for Thermal Decomposition of Ammonium Perchlorate

Qin Liu,‡ [a] Siyu Ma,‡ [b] Xingyang Cui, [a] Shuyue Xu, [a] Jinchao Ma,* [a] Hua Qian* [a]

[a] School of Chemistry and Chemical Engineering, Nanjing University of Science and Technology, Nanjing 210094, P.R. China
[b] Shanghai Space Propulsion Technology Research Institute, Shanghai, 201109, P.R. China

∗ Corresponding author.
‡ These authors contributed equally.
E-mail address: mjinchao@njust.edu.cn (J. Ma), qianhua@njust.edu.cn (Hua Qian).

Content

PCN precursor and PCN

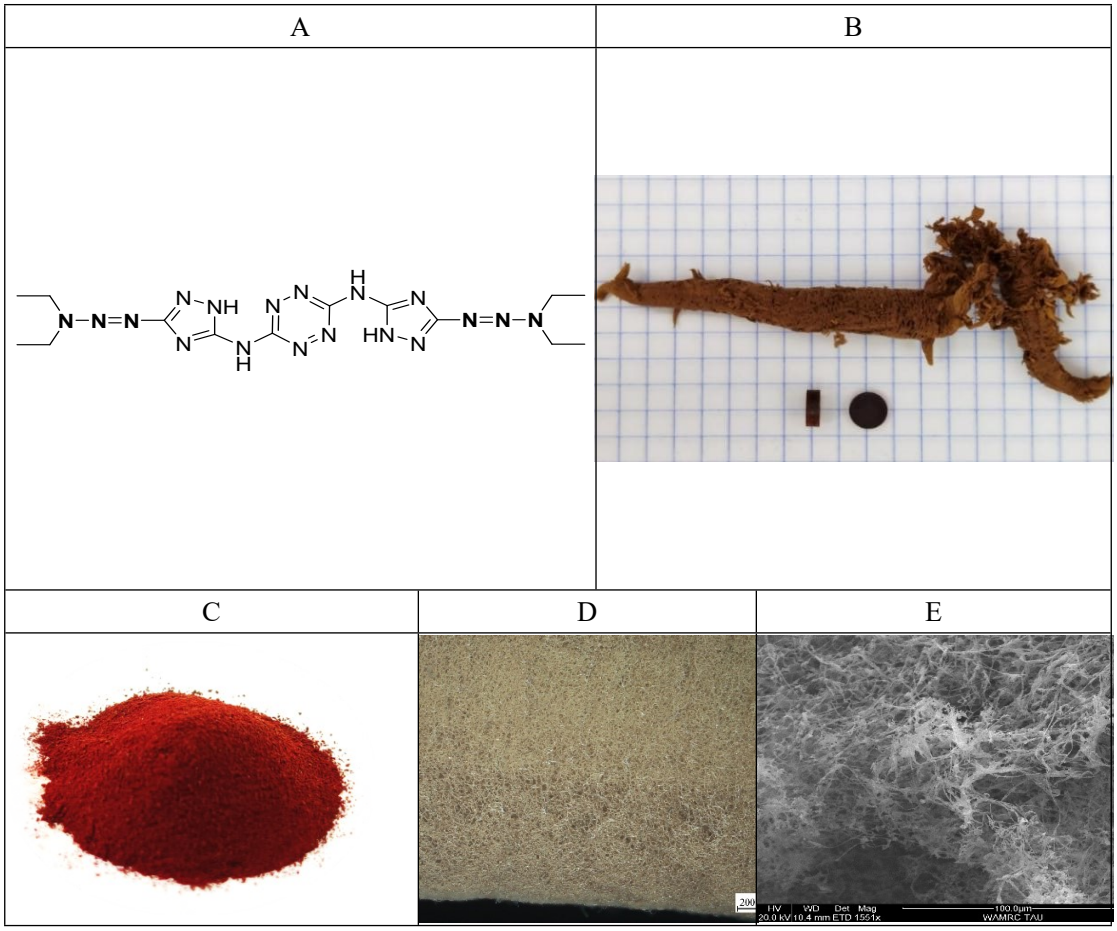

Figure S1. (A) Molecular structure of PCN precursor; (B) comparison diagram of PCN precursor before and after combustion synthesis; (C) powder diagram of PCN precursor; (D) microscope image of PCN; (E) SEM image of PCN.

Characterization of PCN-M composites

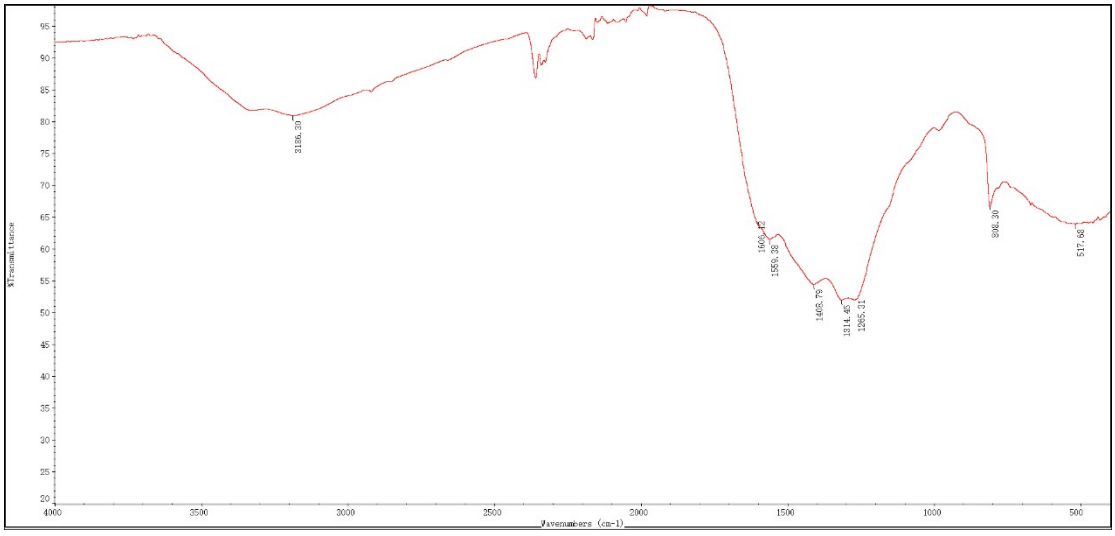

Figure S2. FTIR spectrum of PCN.

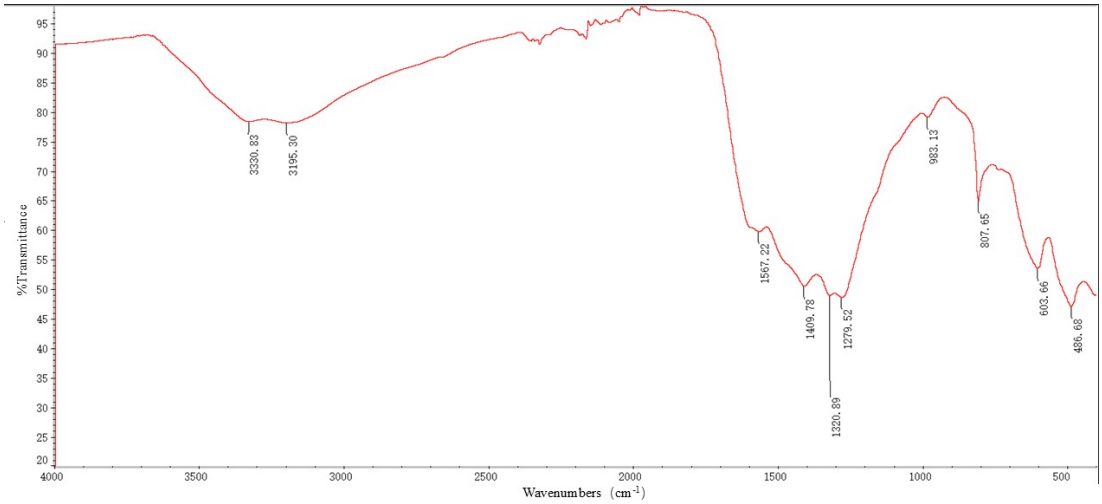

Figure S3. FTIR spectrum of PCN-0.5Mn.

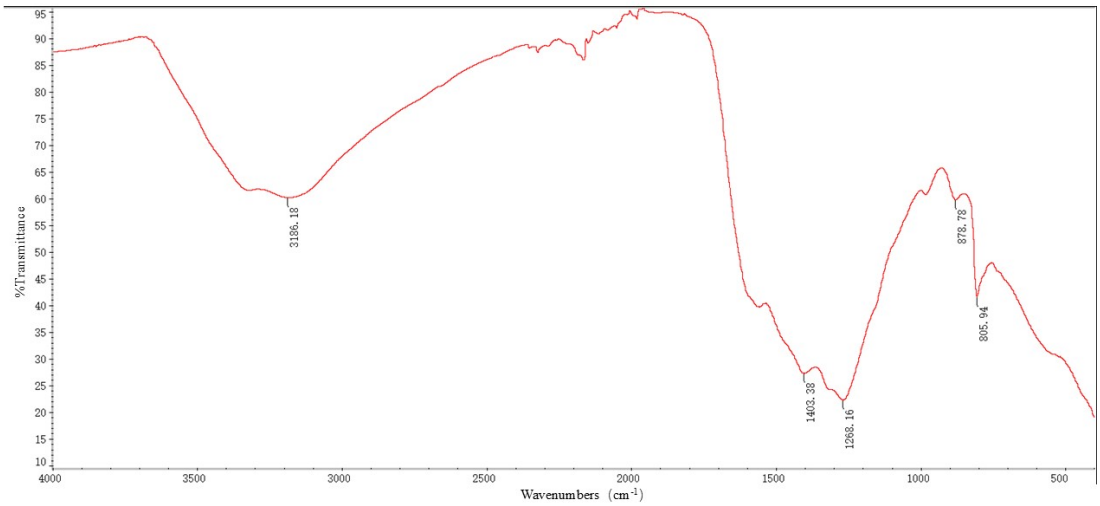

Figure S4. FTIR spectrum of PCN-0.5Fe.

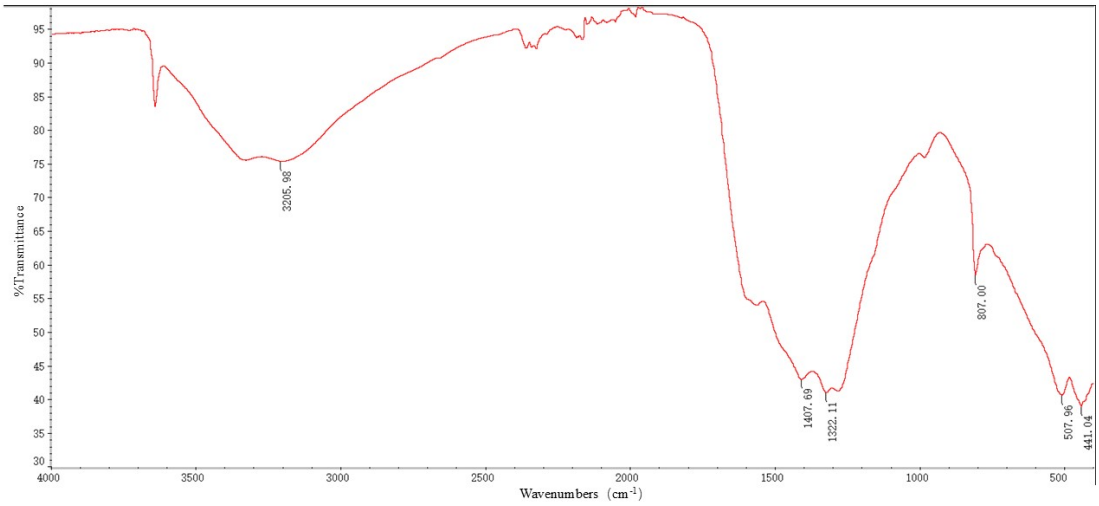

Figure S5. FTIR spectrum of PCN-0.5Ni.

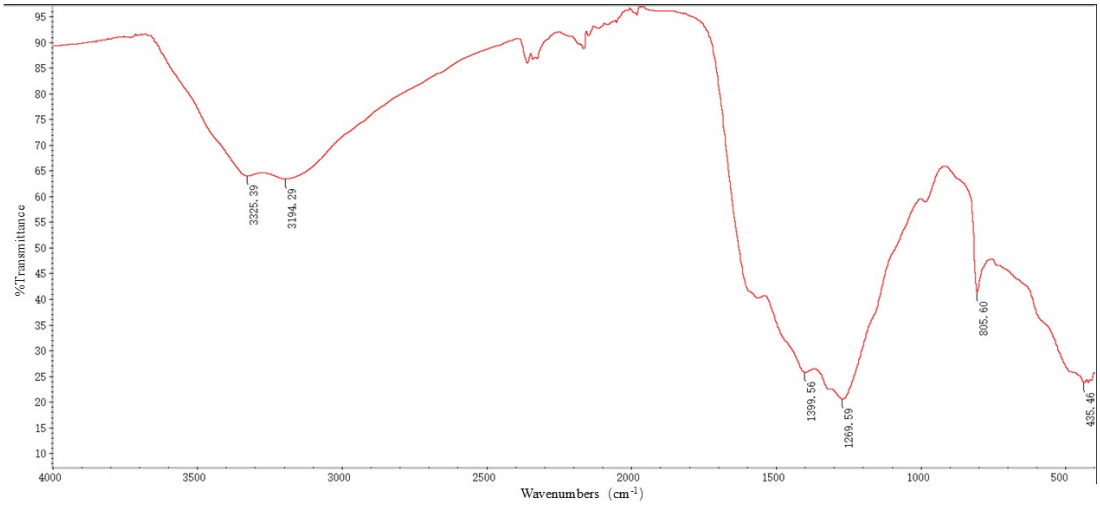

Figure S6. FTIR spectrum of PCN-0.5Cu.

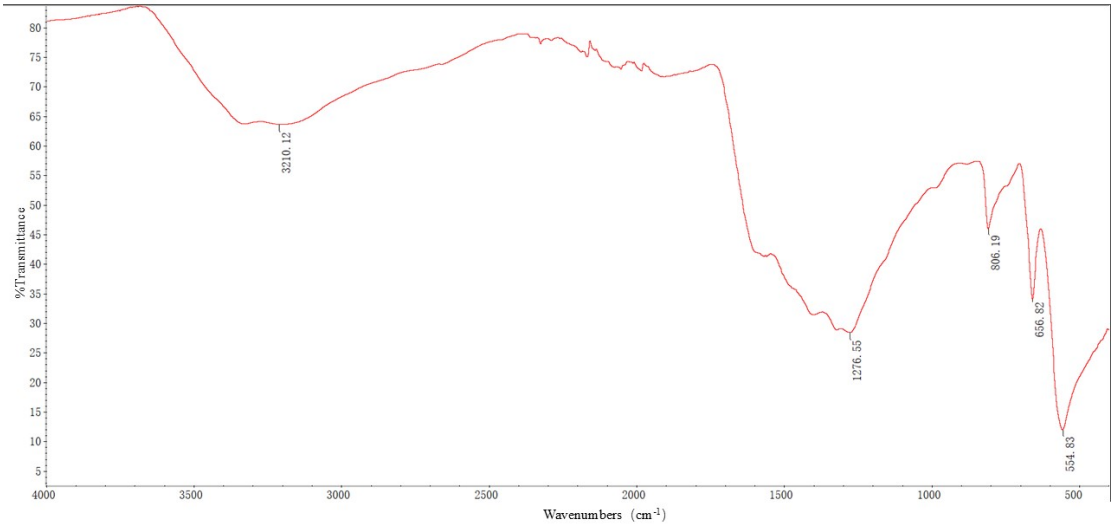

Figure S7. FTIR spectrum of PCN-0.5Co.

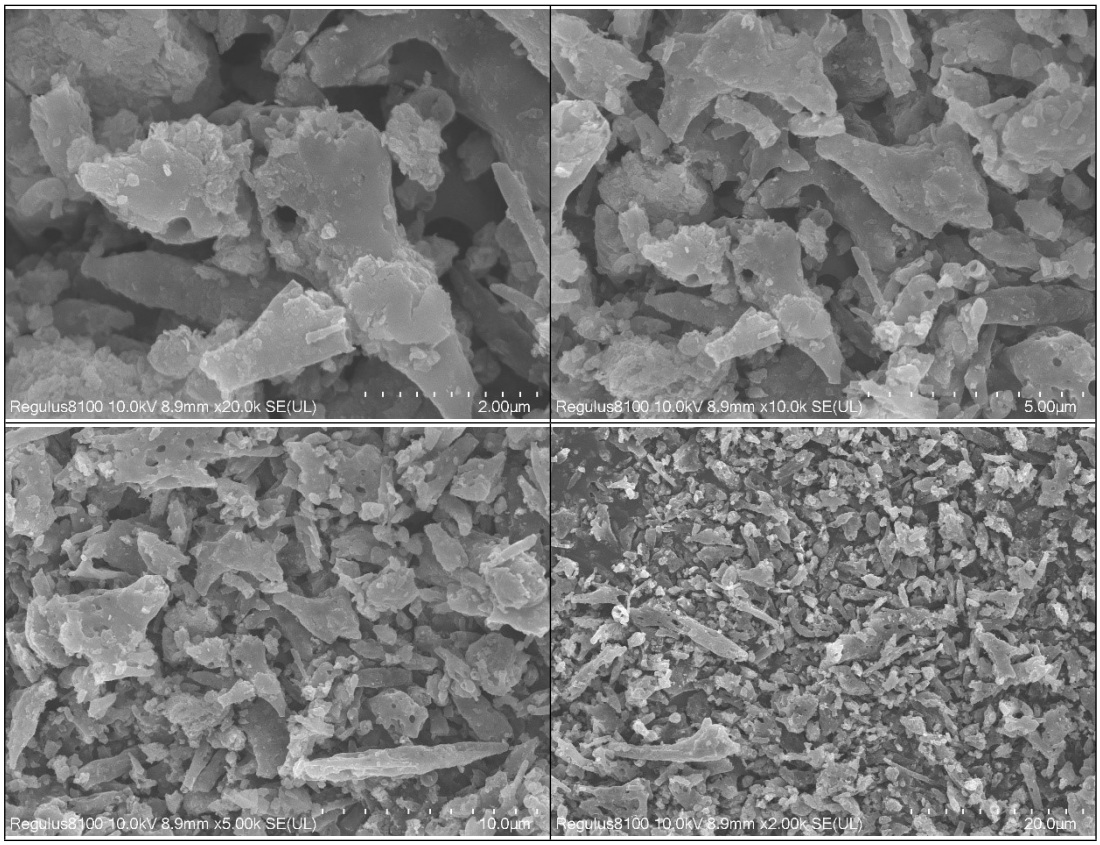

Figure S8. Progressive magnification SEM image of PCN-0.5Co.

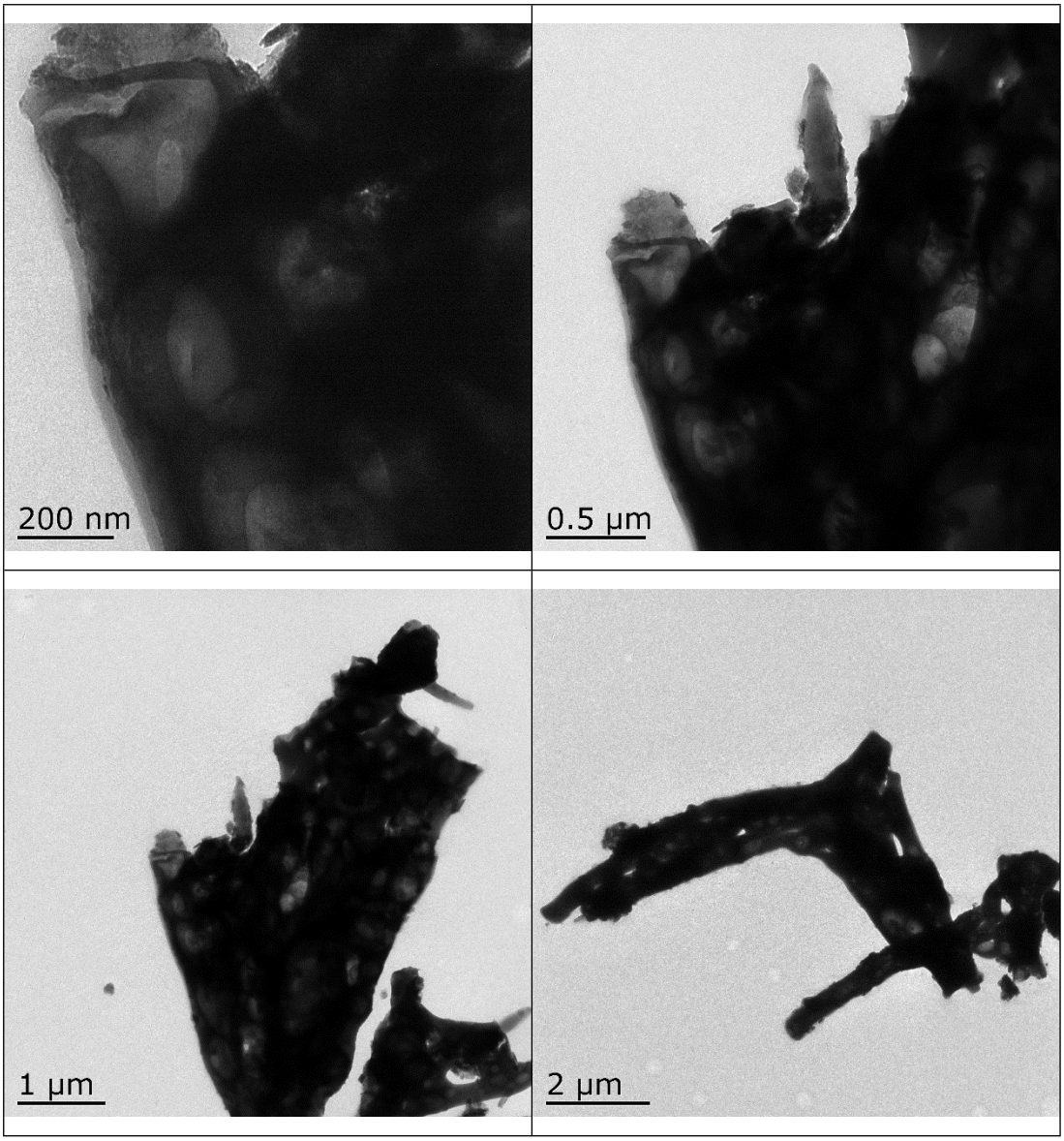

Figure S9. Progressive magnification TEM image of PCN-0.5Co.

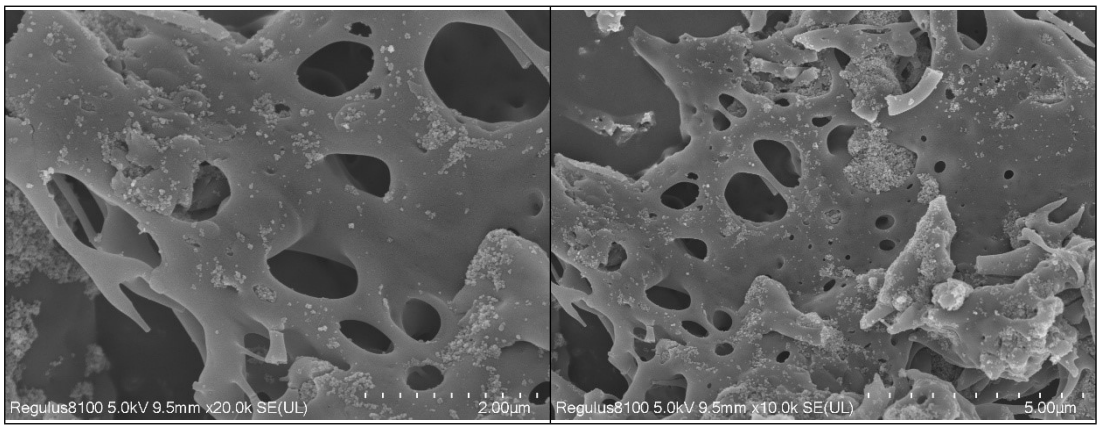

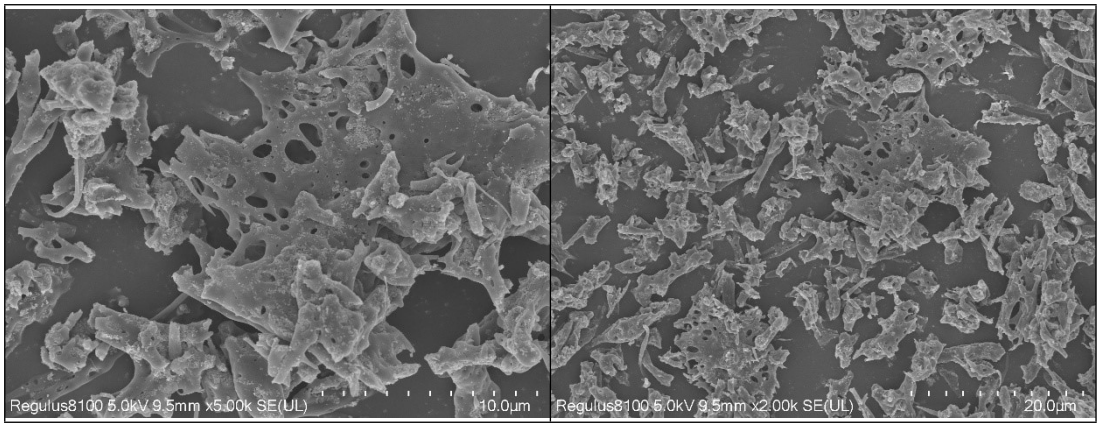

Figure S10. Progressive magnification SEM image of PCN-0.5Mn.

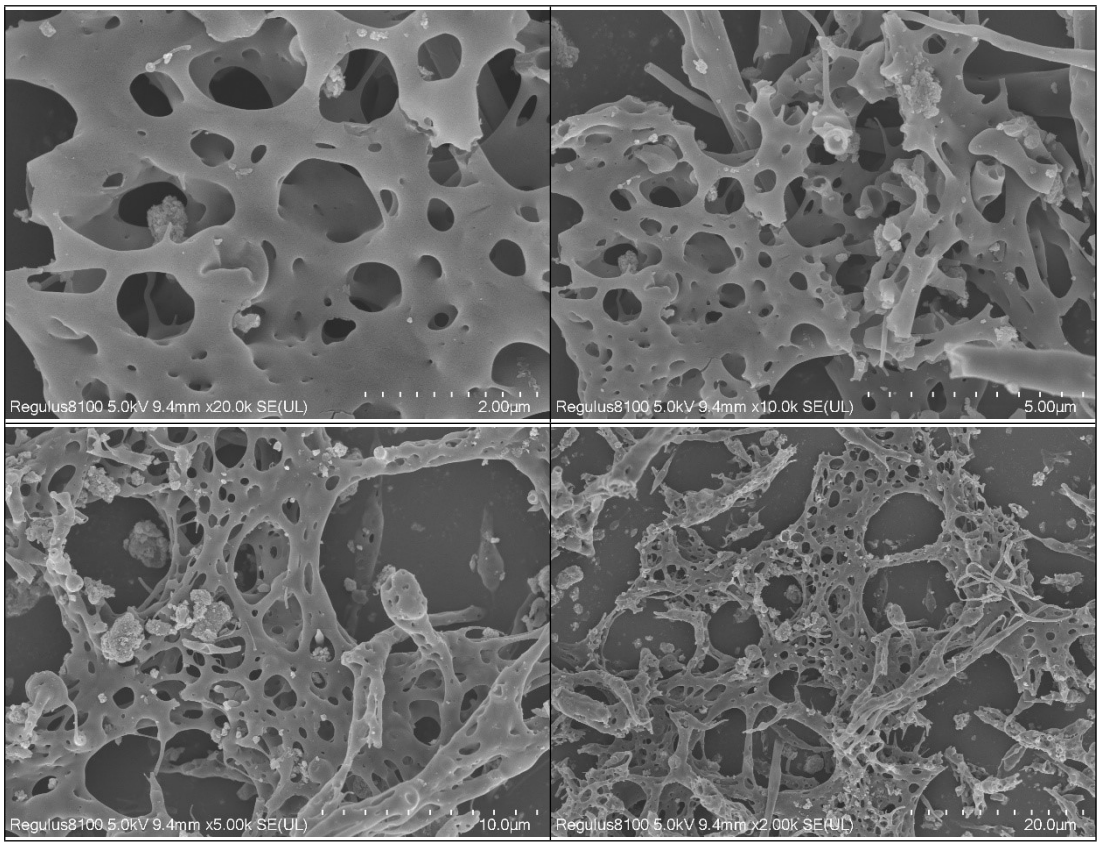

Figure S11. Progressive magnification SEM image of PCN-0.5Fe.

Figure S12.

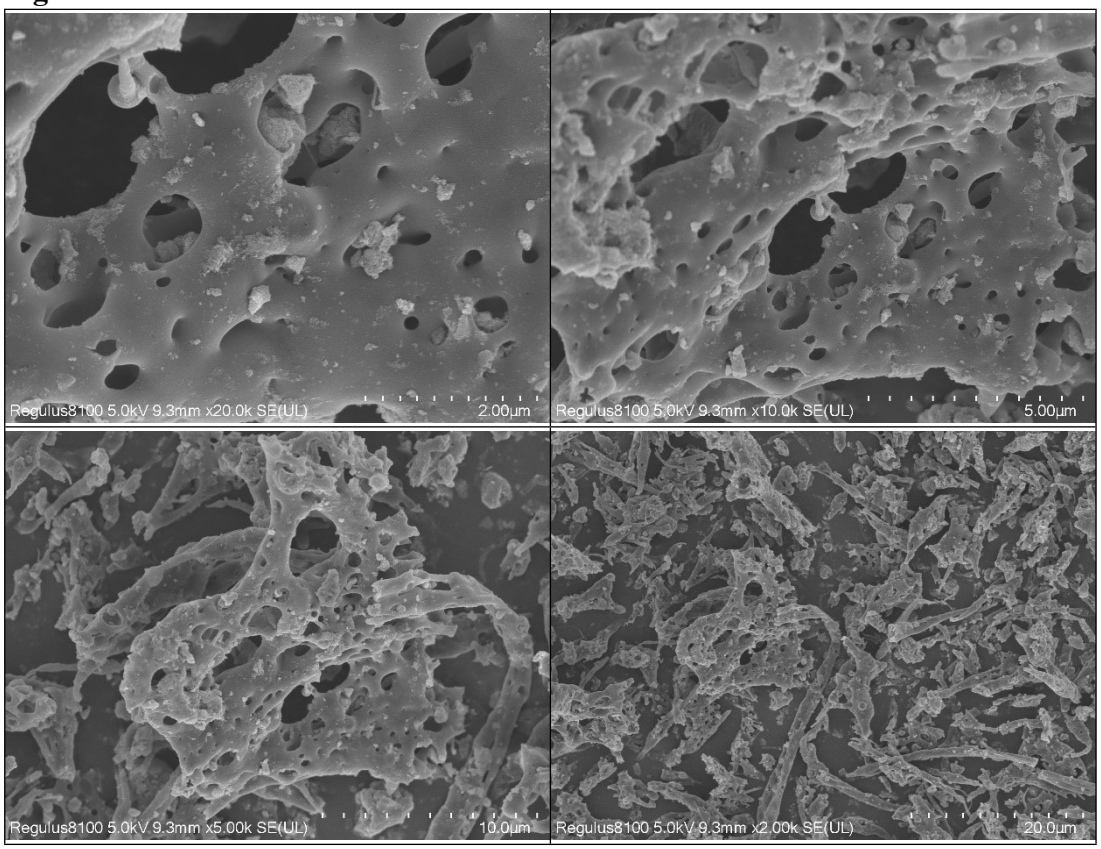

Figure S13. Progressive magnification SEM image of PCN-0.5Ni.

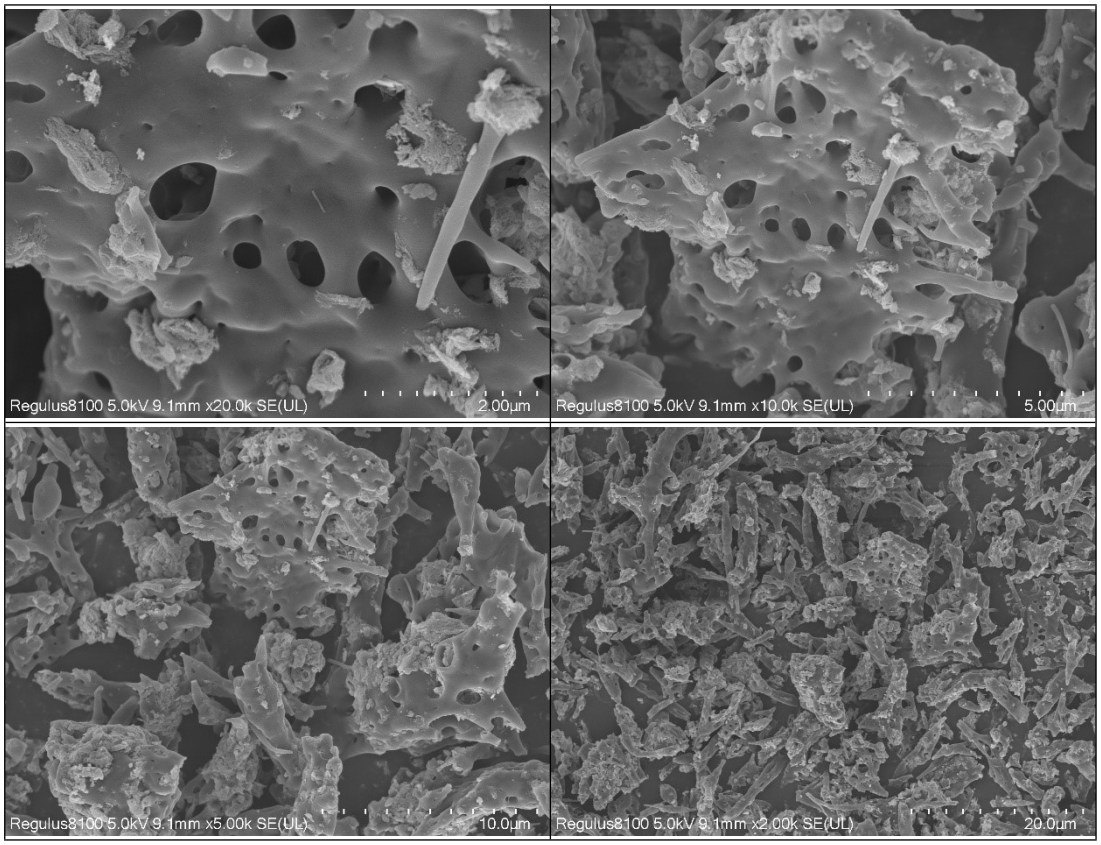

Figure S14. Progressive magnification SEM image of PCN-0.5Cu.

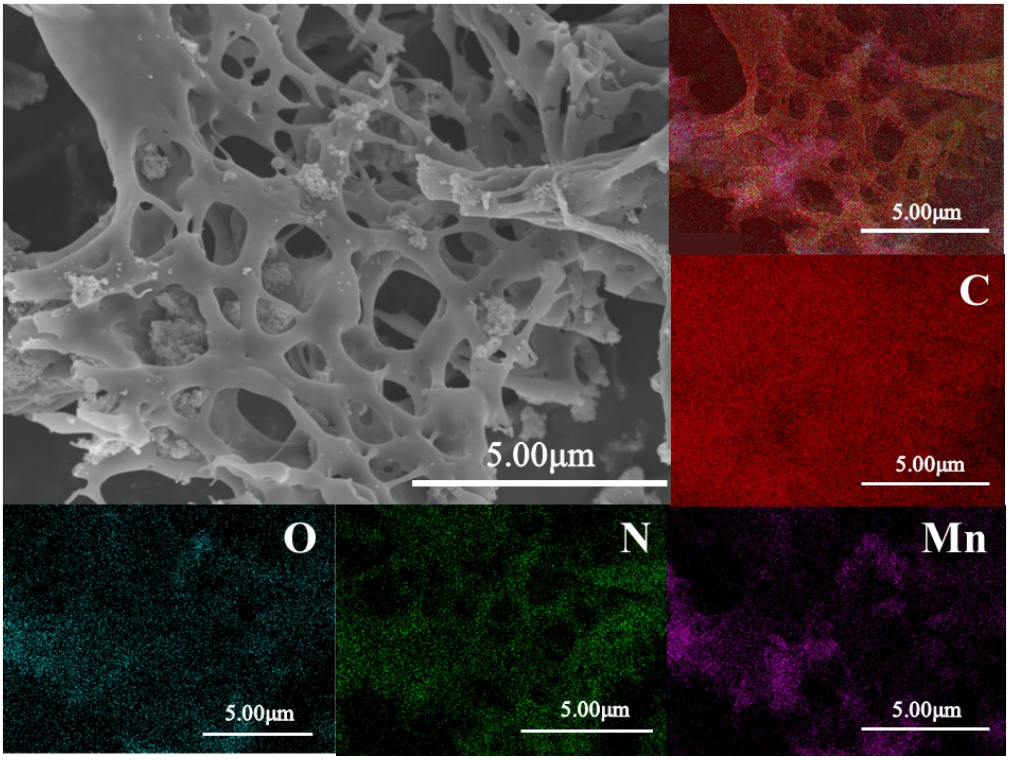

Figure S15. SEM images and elemental map of PCN-0.5Mn.

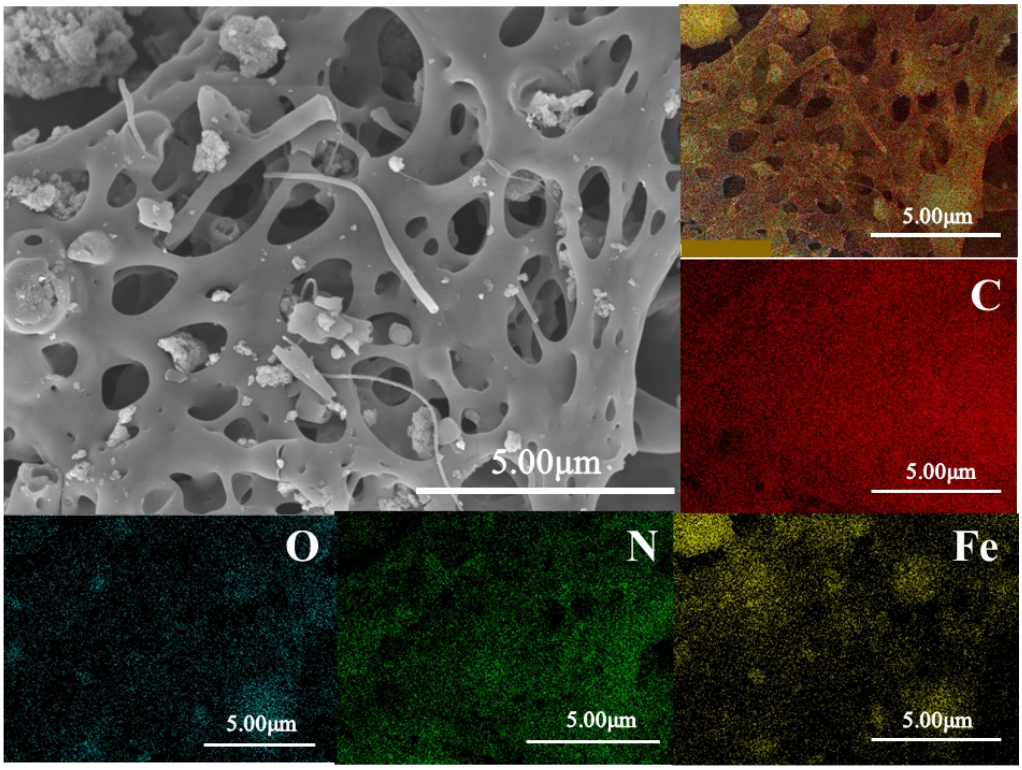

Figure S16. SEM images and elemental map of PCN-0.5Fe.

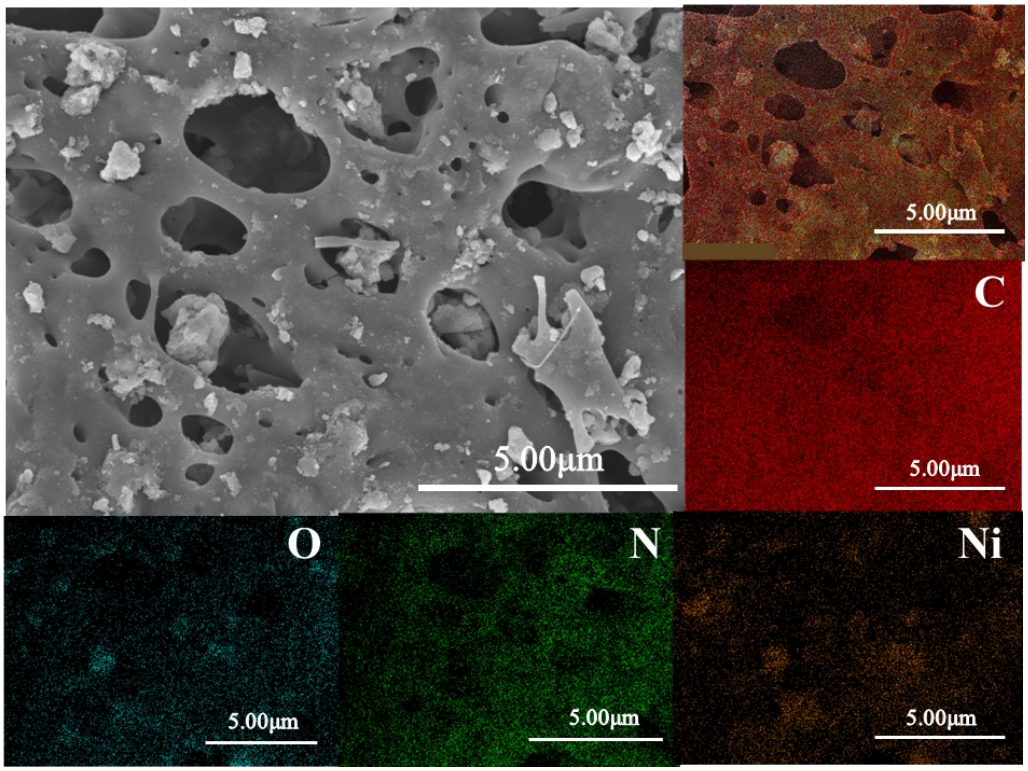

Figure S17. SEM images and elemental map of PCN-0.5Ni.

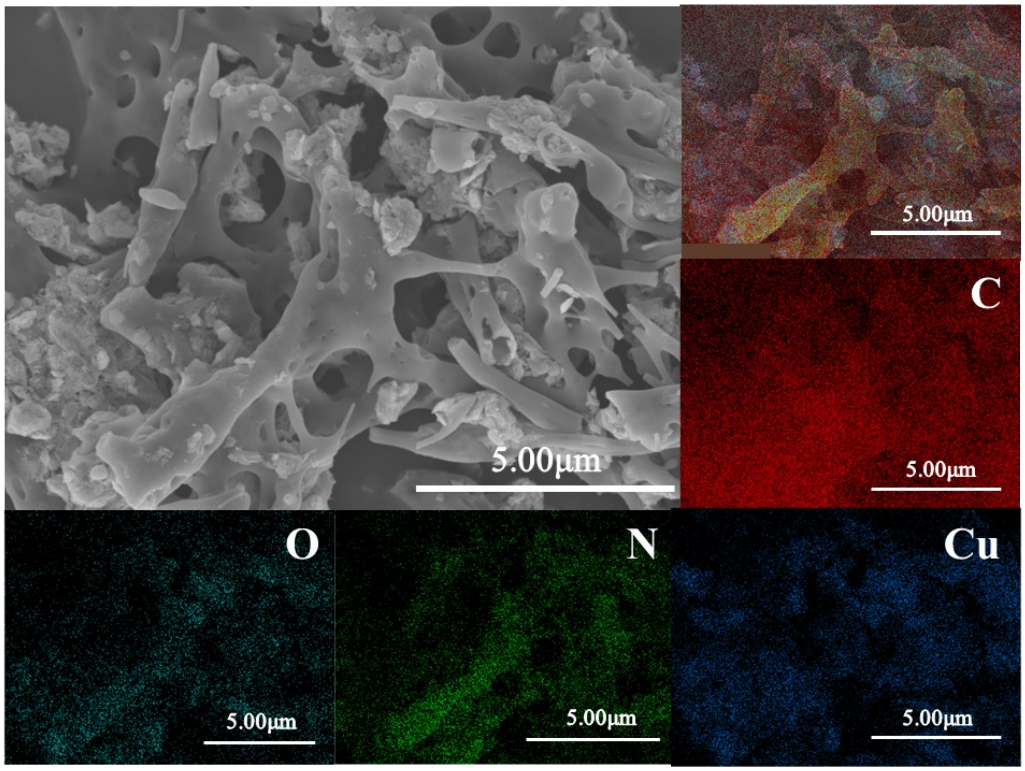

Figure S18. SEM images and elemental map of PCN-0.5Cu.

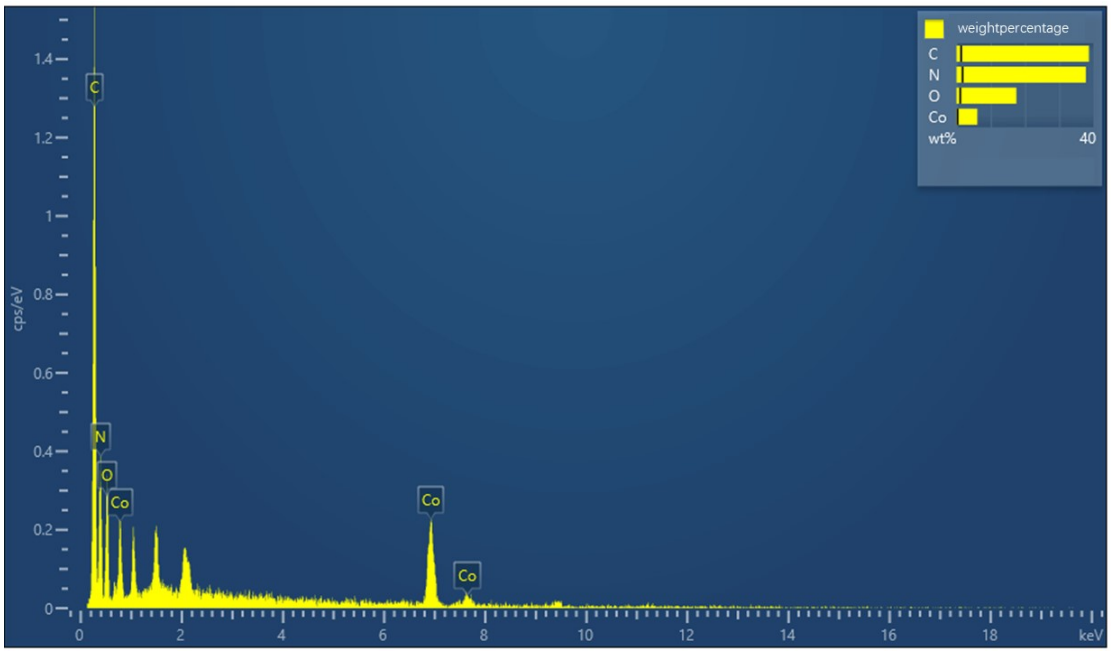

Figure S19. EDS mapping distribution and spectrum of PCN-0.5Co.

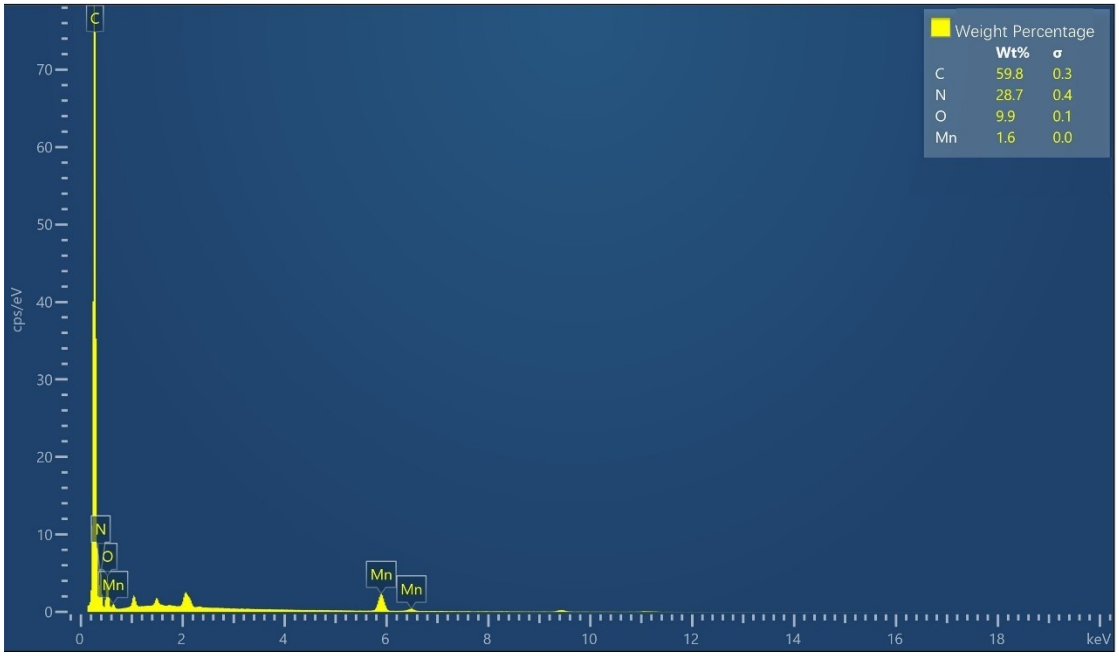

Figure S20. EDS mapping distribution and spectrum of PCN-0.5Mn.

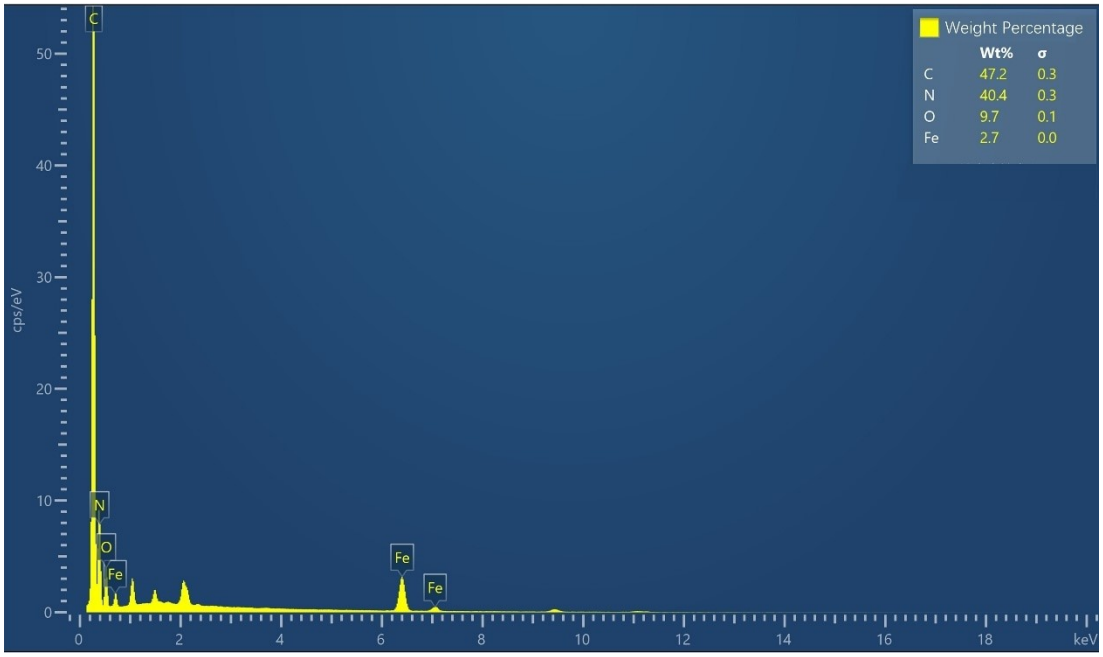

Figure S21. EDS mapping distribution and spectrum of PCN-0.5Fe.

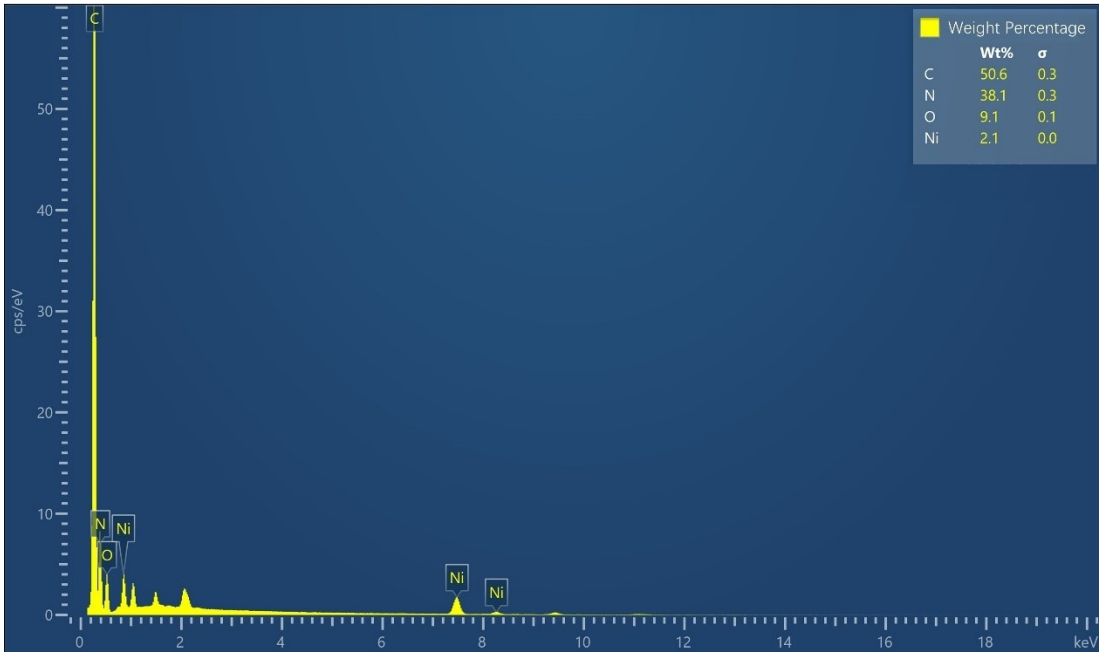

Figure S22. EDS mapping distribution and spectrum of PCN-0.5Ni.

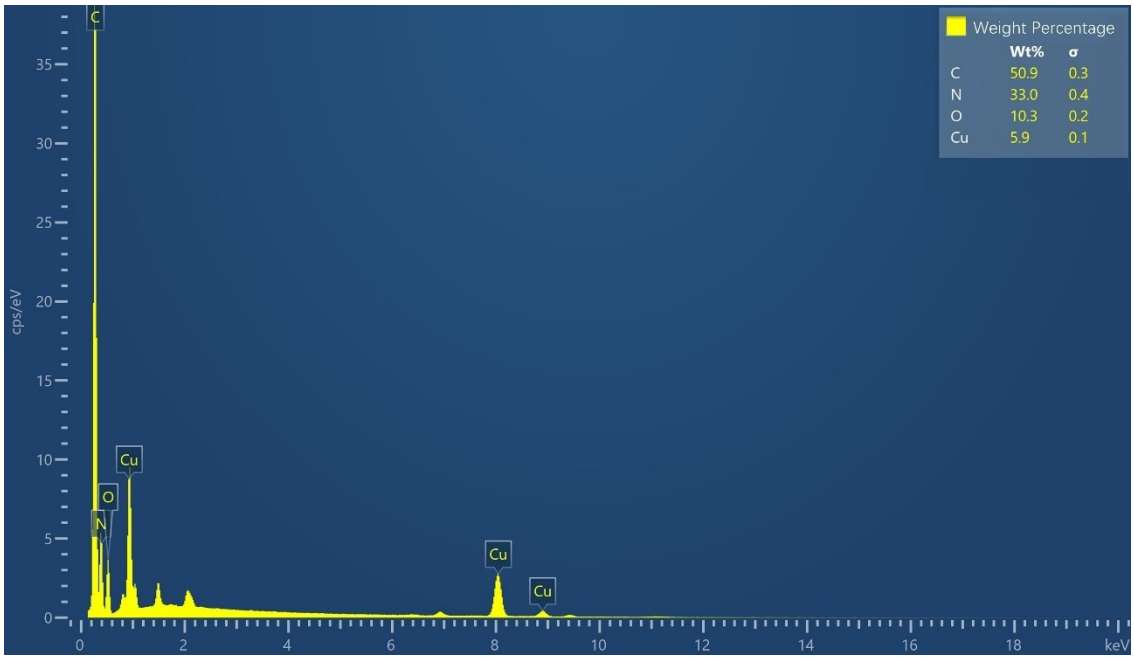

Figure S23. EDS mapping distribution and spectrum of PCN-0.5Cu.

Table S1. Distribution diagram Total spectrum diagram of PCN-0.5Co.

Elements	Series	Apparent concentration	K-ratio	Wt%	Wt% Sigma	At%
C	K-Series	30.07	0.30070	38.67	1.35	45.26
N	K-Series	44.22	0.07872	37.79	1.79	37.93
O	K-Series	9.57	0.03220	17.47	1.11	15.35
Co	K-Series	14.07	0.14065	6.07	0.33	1.45
Gross amount				100.00		100.00

Table S2. Distribution diagram Total spectrum diagram of PCN-0.5Mn.

Elements	Series	Apparent concentration	K-ratio	Wt%	Wt% Sigma	At%
C	K-Series	129.64	1.29645	59.75	0.33	64.84
N	K-Series	44.52	0.07926	28.66	0.37	26.67
O	K-Series	10.22	0.03438	9.95	0.15	8.11
Mn	K-Series	7.84	0.07839	1.63	0.02	0.39
Gross amount				100.00		100.00

Table S3. Distribution diagram Total spectrum diagram of PCN-0.5Fe.

Elements	Series	Apparent concentration	K-ratio	Wt%	Wt% Sigma	At%
C	K-Series	97.23	0.97230	47.20	0.26	52.61
N	K-Series	84.86	0.15108	40.44	0.30	38.65
O	K-Series	9.96	0.03351	9.66	0.15	8.09
Fe	K-Series	13.88	0.13880	2.71	0.03	0.65
Gross amount				100.00		100.00

Table S4. Distribution diagram Total spectrum diagram of PCN-0.5Ni.

Elements	Series	Apparent concentration	K-ratio	Wt%	Wt% Sigma	At%
C	K-Series	105.01	1.05014	50.63	0.27	55.88
N	K-Series	73.66	0.13114	38.11	0.32	36.07
O	K-Series	9.34	0.03145	9.15	0.14	7.58
Ni	K-Series	10.84	0.10837	2.11	0.03	0.48
Gross amount				100.00		100.00

Table S5. Distribution diagram Total spectrum diagram of PCN-0.5Cu.

Elements	Series	Apparent concentration	K-ratio	Wt%	Wt% Sigma	At%
C	K-Series	77.04	0.77044	50.91	0.31	57.85
N	K-Series	53.99	0.09612	32.98	0.38	32.14
O	K-Series	9.78	0.03290	10.25	0.16	8.75
Cu	K-Series	24.73	0.24735	5.87	0.06	1.26
Gross amount				100.00		100.00

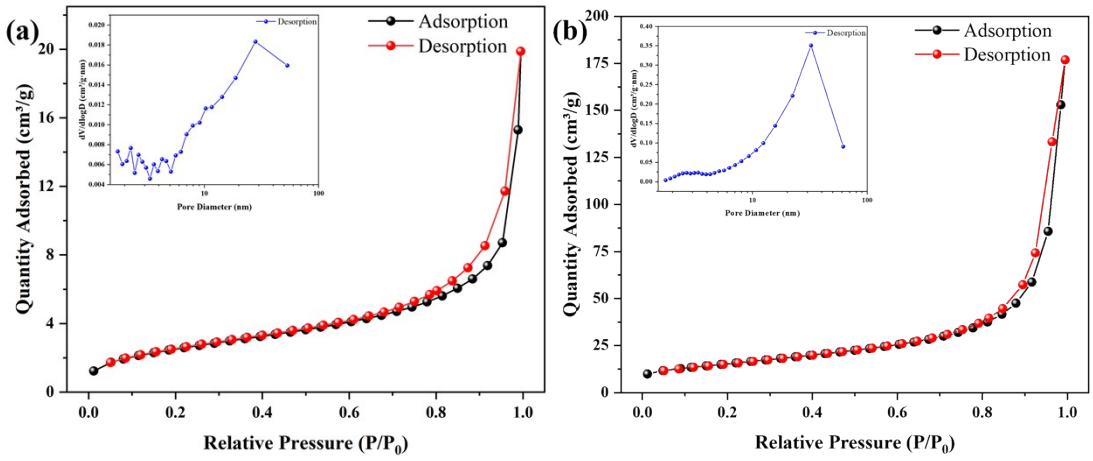

Figure S24. (a)N2 adsorption-desorption isotherm and pore size distribution of PCN; (b) N2 adsorption-desorption isotherm and pore size distribution of PCN-0.5Co

Table S6. BET report for PCN and PCN-0.5Co.

Samples	$S_{BET}(m^2 \cdot g^{-1})$	Pore volume ($cm^3 \cdot g^{-1}$)	Average pore size (nm)	Most Frequent Pore Diameter (nm)
PCN	9.200	0.031	13.477	0.793
PCN-0.5Co	54.811	0.274	20.581	0.790

Promotion of thermal decomposition of AP

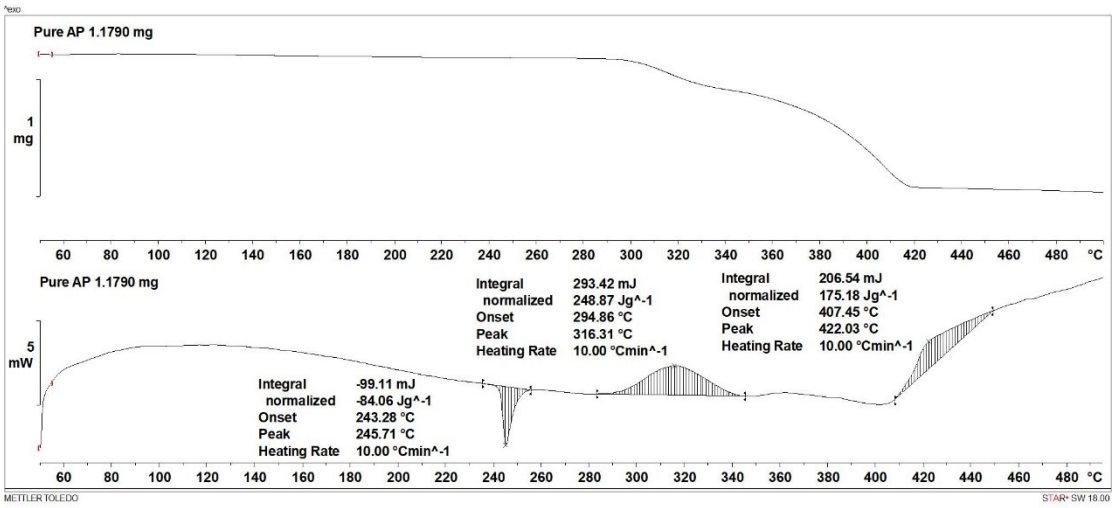

Figure S25. TG and DSC thermograms of pure AP.

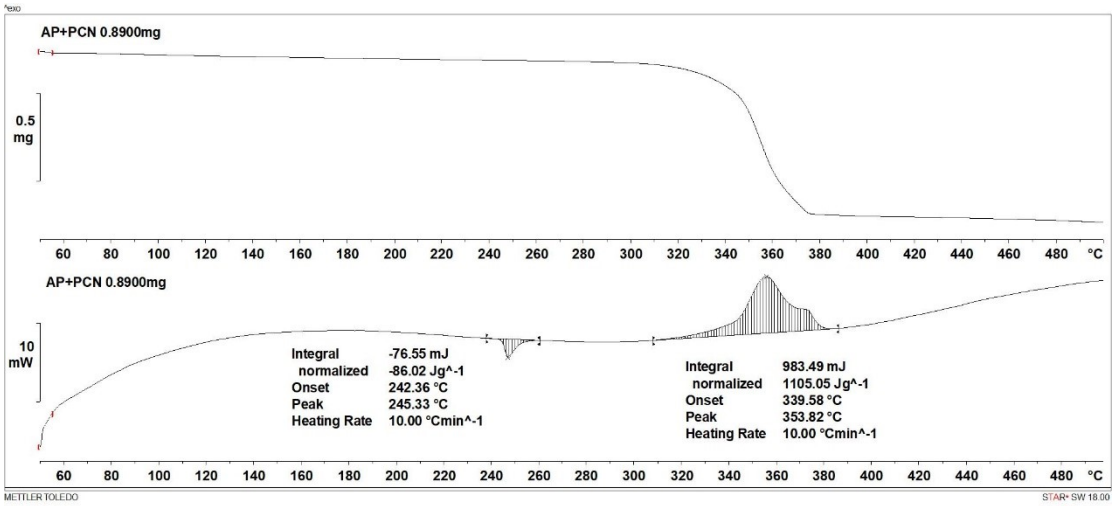

Figure S26. TG and DSC thermograms of AP+PCN.

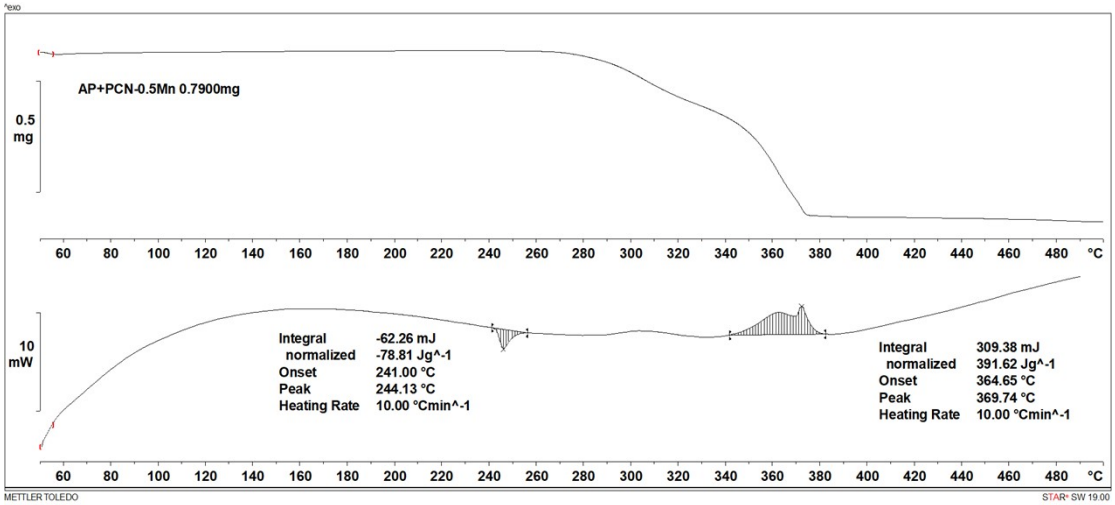

Figure S27. TG and DSC thermograms of AP+PCN-0.5Mn.

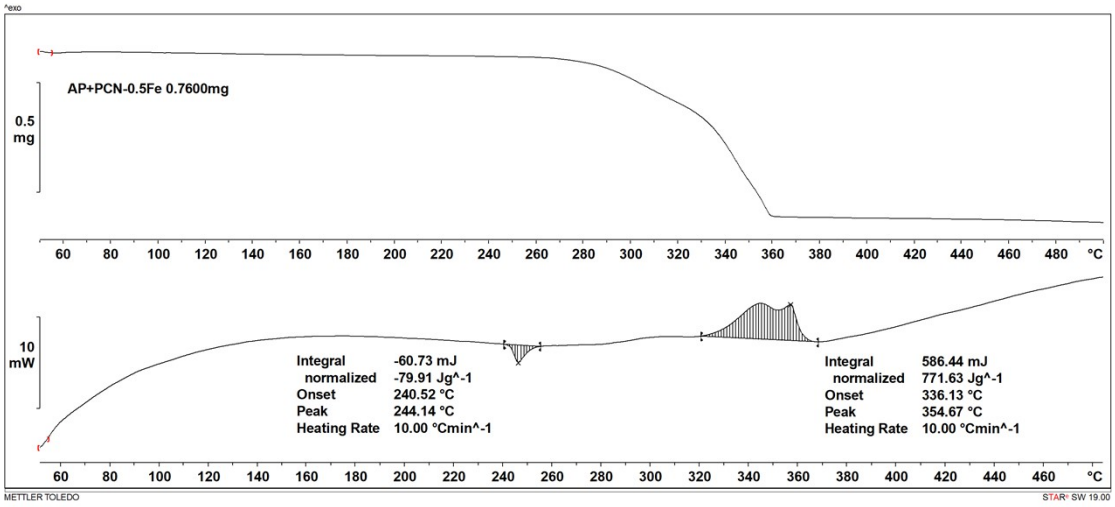

Figure S28. TG and DSC thermograms of AP+PCN-0.5Fe.

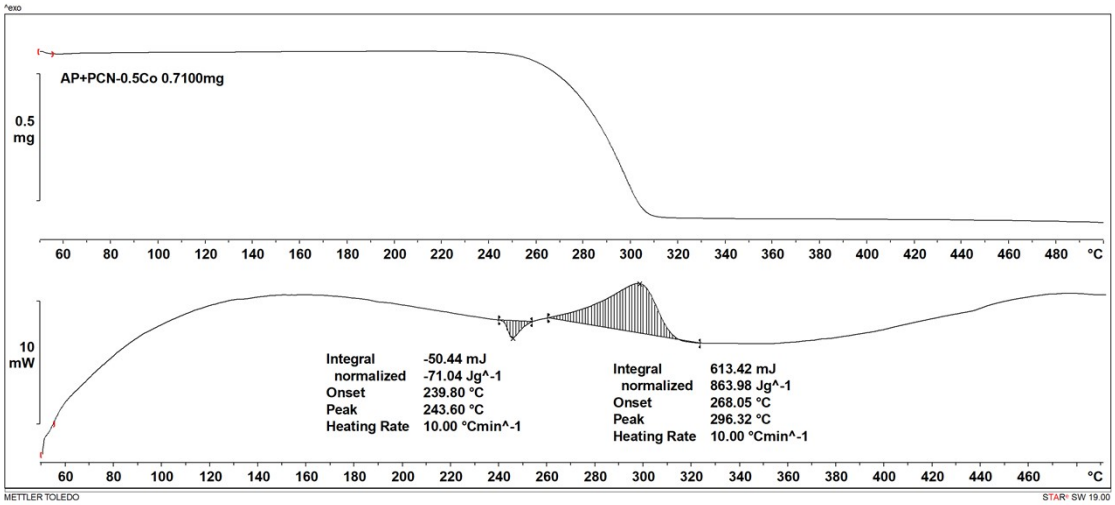

Figure S29. TG and DSC thermograms of AP+PCN-0.5Co.

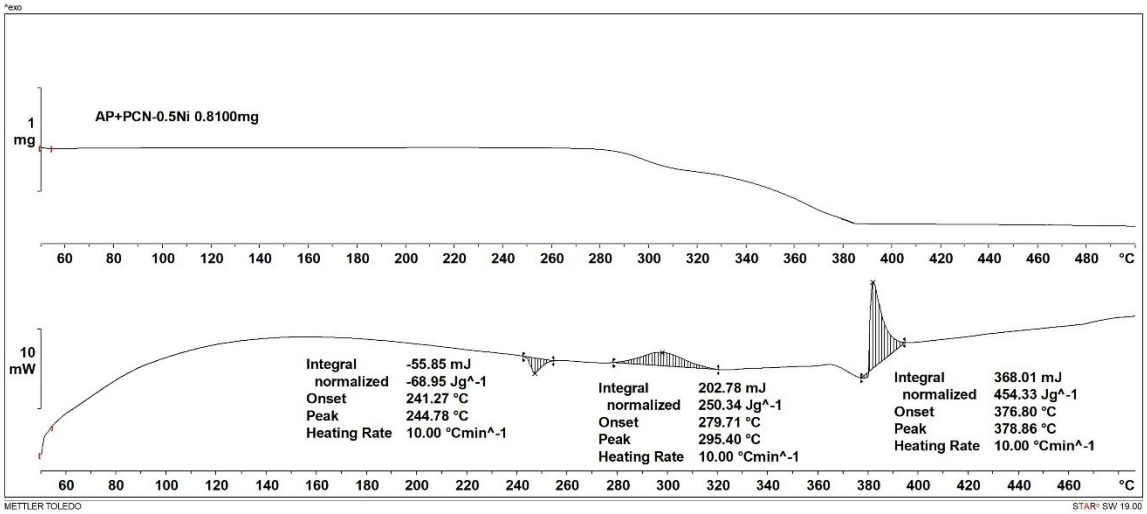

Figure S30. TG and DSC thermograms of AP+PCN-0.5Ni.

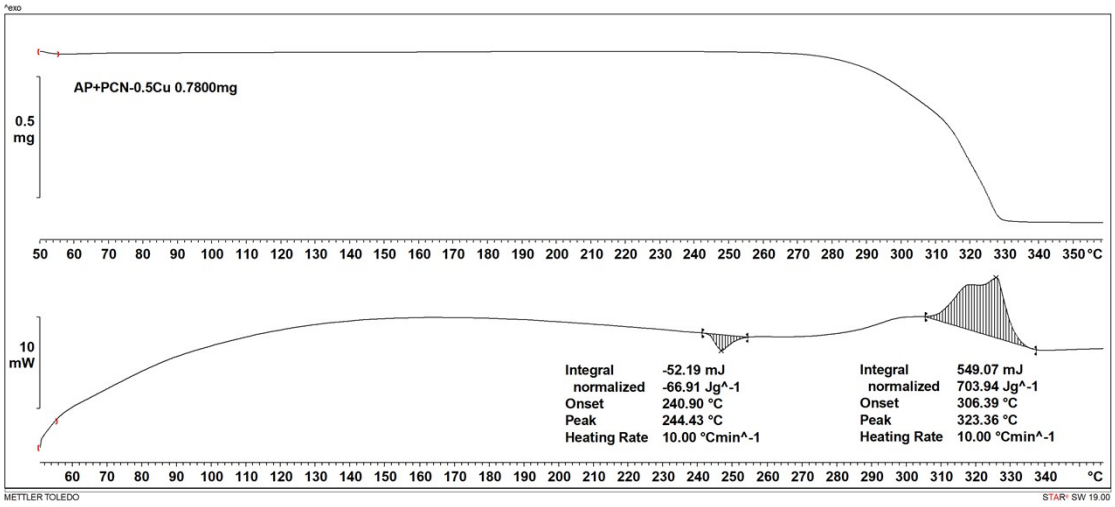

Figure S31. TG and DSC thermograms of AP+PCN-0.5Cu.

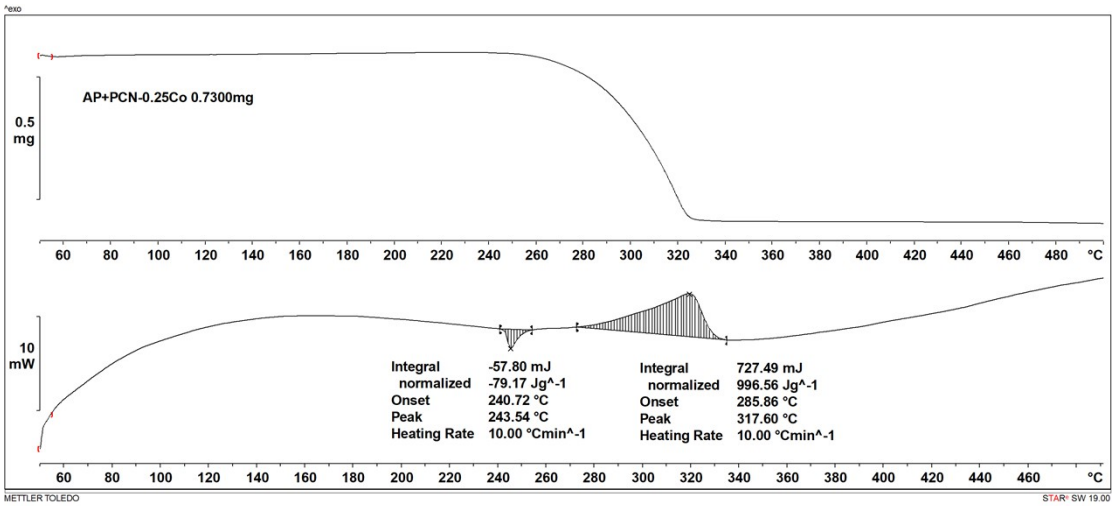

Figure S32. TG and DSC thermograms of AP+PCN-0.25Co.

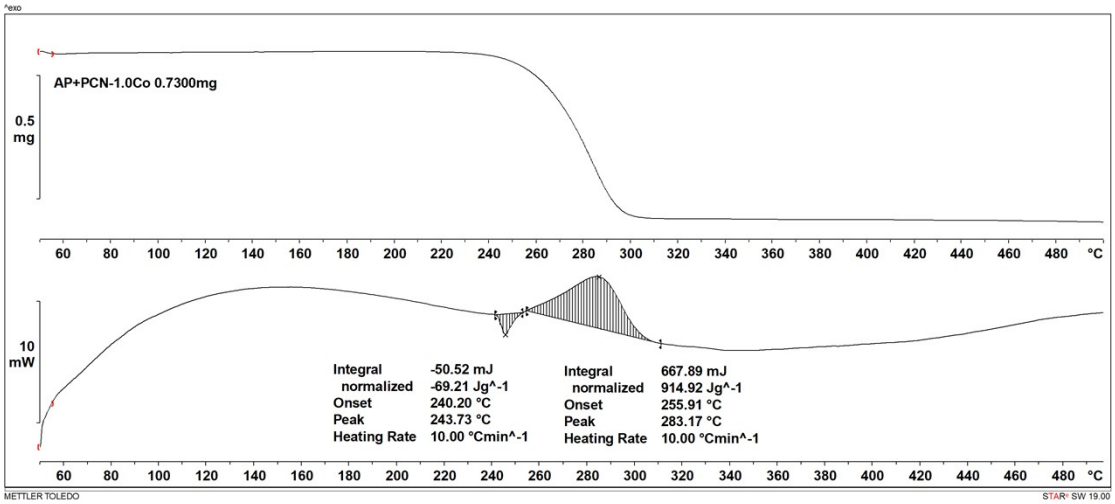

Figure S33. TG and DSC thermograms of AP+PCN-1.0Co.

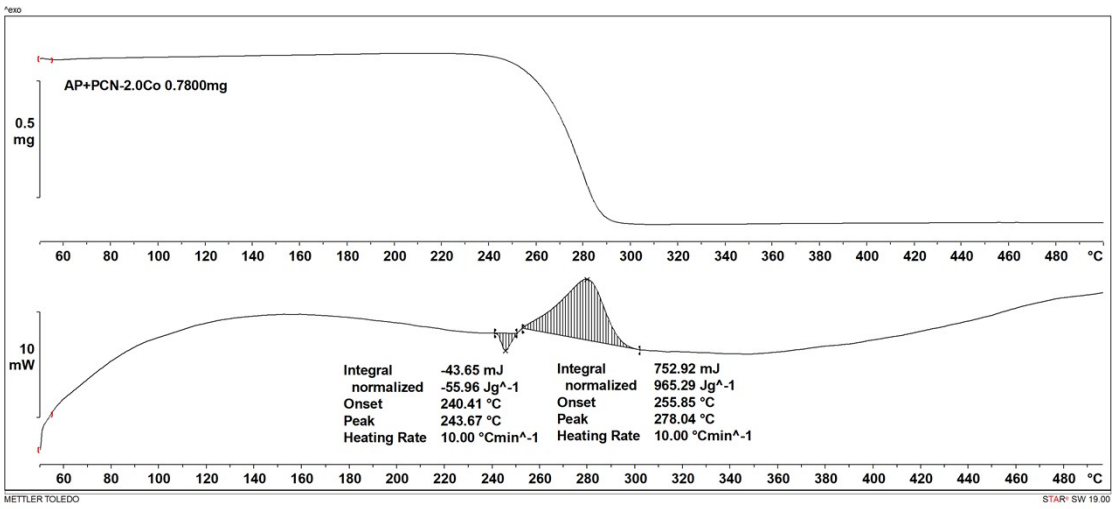

Figure S34. TG and DSC thermograms of AP+PCN-2.0Co.

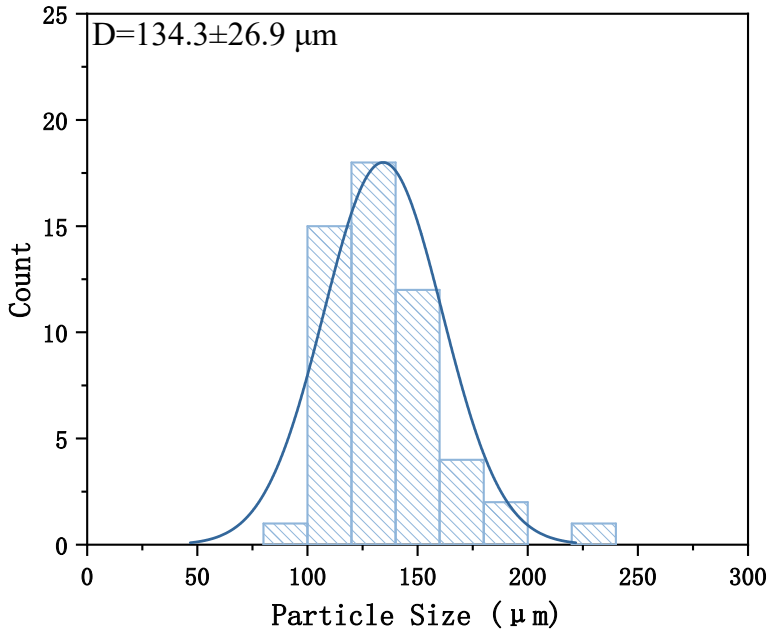

Figure S35. The particle size of the AP.

Table S7. Data of DTG/DSC analysis of AP with and without catalyst.

Sample	T_{LTD}/°C [a]	T_{HTD}/°C [b]	ΔT_{HTD}/°C [c]	Time/min [d]	Q/(J/g) [e]
Pure AP	316.31	422.03		13.96	397.65
PCN	—	353.82	-68.21	9.27	1104.93
PCN-0.5Mn	301.75	369.74	-52.29	12.10	517.36
PCN-0.5Fe	342.10	358.00	-64.03	10.75	1088.01
PCN-0.5Co	—	296.32	-125.71	7.66	988.19
PCN-0.5Ni	298.22	373.56	-48.47	10.89	446.55
PCN-0.5Cu	—	325.36	-96.67	7.83	1342.9
nano-Co_3O_4	—	315.12	-106.91	9.30	592.44
PCN-0.25Co	—	317.60	-104.43	9.82	987.18
PCN-0.5Co	—	296.32	-125.71	7.66	988.19
PCN-1.0Co	—	283.17	-138.86	7.23	947.96
PCN-2.0Co	—	278.04	-143.99	6.70	949.99

[a] Low temperature thermal decomposition temperature; [b] High temperature thermal decomposition temperature; [c] ΔT_{HTD} is the decrease of peak onset temperature; [d] Time to thermal decomposition; [e] Heat released.

Table S8. Comparison of E_a by different catalysts on the thermal decomposition of AP.

Samples		5 K/min	10 K/min	15 K/min	20 K/min	R^2	E_a (kJ/mol)	Sum E_a (kJ/mol)
AP	LTD	293.85	309.20	319.20	324.84	0.9987	114.81	270.43
	HTD	398.63	415.40	425.91	430.29	0.9931	155.62	
AP+PCN	HTD	330.55	343.59	352.87	360.27	0.9962	138.48	138.48
AP+PCN-0.5Mn	LTD	288.65	310.29	322.71	332.25	0.9997	80.34	230.13
	HTD	347.43	361.34	368.52	377.01	0.9937	149.79	
AP+PCN-0.5Fe	LTD	315.53	323.43	329.27	331.84	0.9960	235.45	368.80
	HTD	343.43	357.08	368.36	375.03	0.9950	133.35	
AP+PCN-0.5Co	HTD	301.08	315.50	327.75	332.67	0.9926	113.04	113.04
AP+PCN-0.5Ni	LTD	291.21	306.39	316.24	321.68	0.9984	115.59	325.16
	HTD	375.14	384.58	392.58	397.61	0.9931	209.57	
AP+PCN-0.5Cu	HTD	313.47	325.27	331.84	336.76	0.9996	167.26	167.26

Characterization of solid propellants

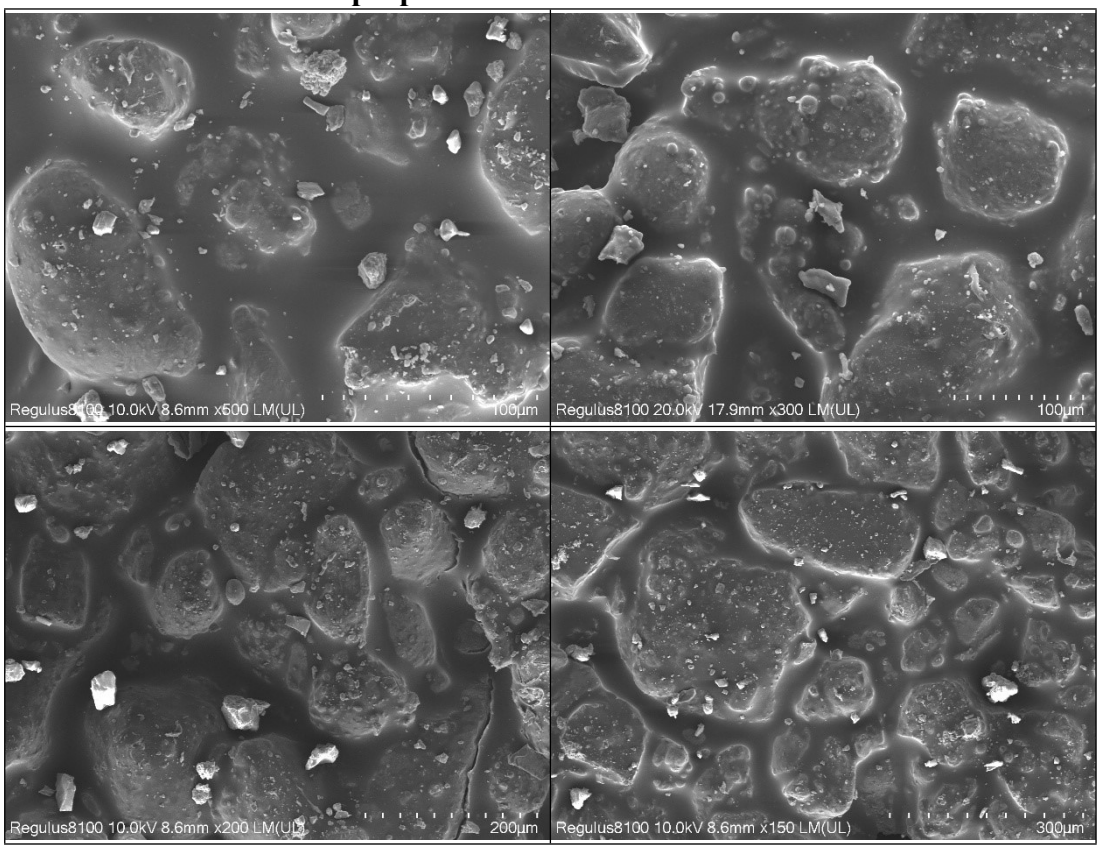

Figure S36. Progressive magnification SEM image of HTPB-based solid propellant with PCN-2.0Co (2 wt.%).

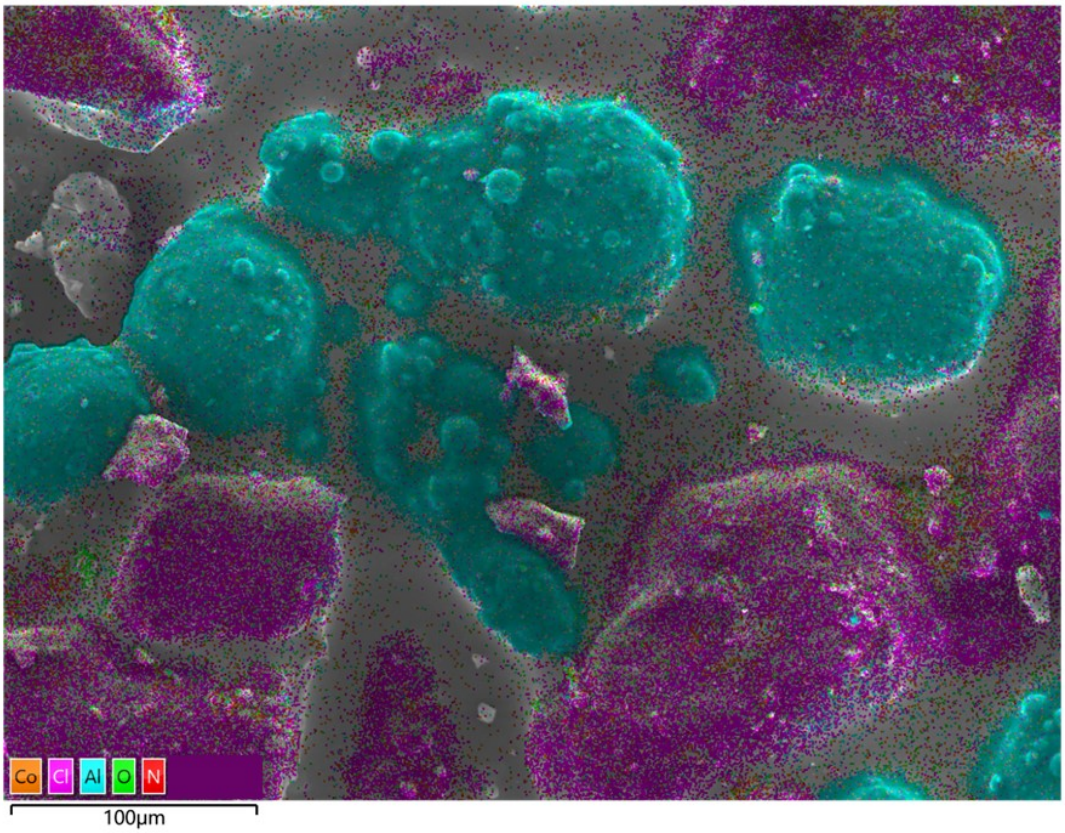

Figure S37. EDS mapping distribution and spectrum of HTPB-based solid propellants with PCN-2.0Co (2 wt.%).

Table S9. Distribution diagram Total spectrum diagram of HTPB-based solid propellants with PCN-2.0Co (2 wt.%).

Elements	Series	Apparent concentration	K-ratio	Wt%	Wt% Sigma	At%
N	K-Series	1.20	0.00213	3.03	0.63	5.02
O	K-Series	11.14	0.03748	28.33	0.26	41.06
Al	K-Series	42.98	0.30867	47.94	0.34	41.20
Cl	K-Series	12.70	0.11099	17.58	0.14	11.50
Co	K-Series	2.53	0.02529	3.12	0.07	1.23
Gross amount				100.00		100.00

Table S10. Physical and combustion properties of HTPB-based solid propellants without and with 2wt.% additives.

	Without additive	Ferrocene derivative	Nano-Co_3O_4	PCN precursor	PCN	PCN-2.0Co
T_{LTD}/℃	300.1	—	300.49	301.42	311.17	—
T_{HTD}/℃	380.68	355.17	343.83	372.42	387.83	327.17
ΔT_{HTD}/℃		-25.51	-36.85	-8.26	7.15	-53.51
ρ/g·cm^{-3}	1.52	1.54	1.53	1.51	1.53	1.52
Q_V/J·g^{-1}[a]	4954	4971	5090	4837	4922	4996
Impact/J[b]	5	6	5	5	8	7
Friction/N[c]	252	288	252	288	>360	360
Burning rate/mm·s^{-1}	0.972	1.013	1.265	1.084	0.953	1.355

[a] The heat of explosion was measured under a 3 MPa Ar atmosphere; [b] The impact sensitivity of the sample was tested using the BAM fall hammer impact sensitivity tester (IDEA SCIENCE BFH 20). [c] The friction sensitivity of the sample was tested using the BAM friction sensitivity tester (IDEA SCIENCE FST 20).

Composition and Burning Rate	PCN (2wt.%) 0.953 mm·s^{-1} 3.65↓	nano-CuO (2wt.%) 1.265 mm·s^{-1} 30.14%↑	Ferrocene derivative(2wt.%) 1.013mm·s^{-1} 4.21%↑
0 s			
20 s			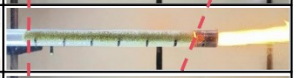
40 s			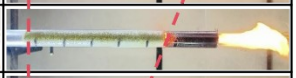
60 s		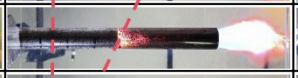	
80 s	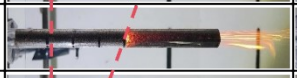		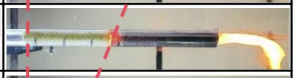
100 s			
120 s			
140 s			

Figure S38. Ignition burn diagrams of HTPB-based solid propellants with different types of catalysts added.